

## **THE IMPACT ANALYSIS OF LATERAL RESTRAINT ON THE STATE OF STRESS AND STRAIN IN THE THIN-WALLED Z-SECTION BEAM**

### **Summary**

The behaviour of thin-walled Z-section beam subjected to gravity load for different variants of lateral restraints is analyzed. For the basic variant of the laterally restrained beam the one defined in Eurocode 3 (EN 1993-1-3:2006) is taken. The Z-section beam which is laterally restrained along the flange by trapezoidal steel sheeting is observed, shown as a Z-section beam laterally restrained with linear stiff connection and rotary elastic connection. Variant of laterally restrained Z-section beam with a linear stiff connection, a variant of laterally restrained Z-section beam with rotary elastic connection and beam without lateral restraints are analyzed. Based on the research, analysis and comparison of the results for individual variants of thin-walled Z-section beams, with and without lateral restraints, is conducted.

*Key words:*        *thin-walled Z-section beam; lateral restraint; linear stiff connection; rotary elastic connection; rotational stiffness*

### **1. Introduction**

Several researchers have investigated the behaviour of the roof purlins and thin walled beams with partial restraints provided by their supported cladding or sheeting [1-4]. The basic technical theory of thin-walled member with open cross-section was developed by Vlasov [5]. He applied the term “sectorial coordinate” for the first time and presented the subject of mixed torsion in a most outstanding manner. The torsion, buckling and bending analysis of thin-walled beams has been elaborated in a great number of studies [6-9]. The attention has been paid also to the laterally restrained thin-walled open cross-section beams [10, 11]. The resistance of beams to lateral instability can be improved through the provision of effective lateral bracing. Lots of studies of lateral restraint requirements have been carried out [12, 13]. Pavazza and Jović gave comparison of analytical and numerical results for the thin-walled beams subjected to bending [14, 15].

The behaviour of thin-walled Z-section beam subjected to gravity load for different variants of lateral restraints is analyzed. The Z-section beam which is laterally restrained along the flange by trapezoidal steel sheeting is taken for the basic variant of laterally restrained beam. This basic variant is defined in Eurocode 3 (EN 1993-1-3:2006) [16]. According to this variant, the model “A” of a thin-walled Z-section beam is laterally

restrained by a linear stiff connection and a rotary elastic connection which replace the lateral restraint of the beam by trapezoidally profiled sheeting. This partial torsional restraint may be represented by a rotational spring of a specified rotational stiffness  $C_D$ , [17] which comprises the rotational stiffness of the connection between the sheeting and the beam, and the rotational stiffness corresponding to the flexural stiffness of the trapezoidal sheeting. Next is the variant of the laterally restrained Z-section beam with linear stiff connection observed (model „B“), variant of the laterally restrained thin-walled Z-section beam with rotary elastic connection with stiffness  $C_D$  (model „C“), and finally the Z-section beam without lateral restraint (model „D“) [18-20].

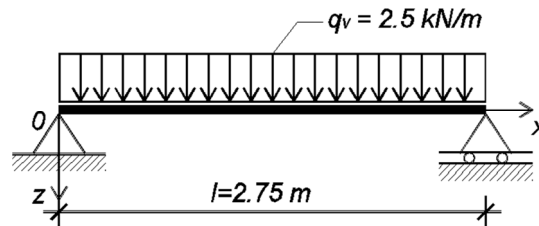


Fig. 1 Beam on two bearings loaded with gravity load  $q_v$

Thereby the freely laid beam on two bearings with span  $l$  is considered, Figure 1. Supports of thin walled beam do not allow the rotation and lateral displacement.

**2. Thin-walled Z-section beam laterally restrained by linear stiff connection and rotary elastic connection (Model “A“)**

A thin-walled Z-section beam laterally restrained in the point H by a linear stiff connection and rotary elastic connection with rotational stiffness  $C_D$  which replace the lateral restraint of the beam by trapezoidally profiled sheeting T 53/162.5/1 is shown in Figure 2.

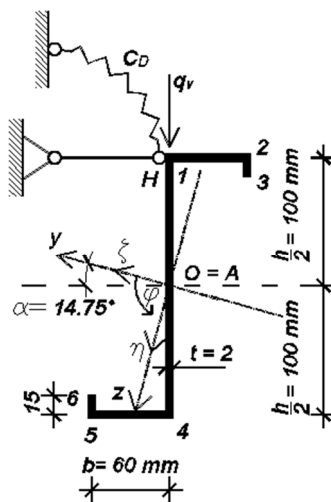


Fig. 2 Thin-walled Z-section beam laterally restrained by linear stiff connection and rotary elastic connection (Model “A“)

The total rotational stiffness of rotational spring  $C_D$ , Fig. 3, is defined according to EN 1993-1-3:2006, section 10.1.5.2. [16]:

$$C_D = \frac{1}{\frac{1}{C_{D,A}} + \frac{1}{C_{D,C}}} \tag{1}$$

The rotational stiffness  $C_{D,A}$  [16] which comprises rotational stiffness of the steel sheeting and beam connection is determined experimentally. The rotational stiffness  $C_{D,C}$  [16] which corresponds to the bending stiffness of trapezoidal steel sheeting can be determined according to the following:

$$C_{D,C} = k \cdot \frac{E \cdot I_{eff}}{s} \quad (2)$$

where:

$I_{eff}$ - effective moment of inertia of the cross section for the unit width of sheet,

$s$  - space between thin-walled beams (span of the sheet),

$k=2$  - for sheets over one field,

$k=4$  - for sheets continuing over two or more fields.

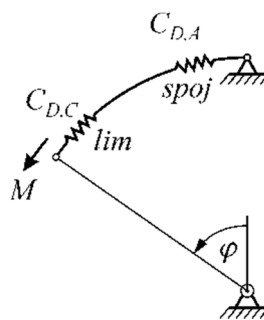


Fig. 3 Model of rotational spring

Axes  $y, z$  are the main inertia axes of the cross-section, while the axis  $x$  is a longitudinal axis of the beam. Point  $A$  is the shear centre and it coincides with the centre of gravity of the cross section. Displacement components of the shear centre  $A$  in the direction of the main axes of inertia  $y$  and  $z$  are marked  $\xi(x)$  and  $\eta(x)$ , while  $\varphi(x)$  is a rotation angle of the cross-section around the axis of the shear centre, Figure 2.

Displacement of the point  $H$  in the direction of a linear stiff connection:

$$\delta_H = \xi \cdot \cos \alpha + \eta \cdot \sin \alpha + \frac{h}{2} \cdot \varphi = 0 \quad (3)$$

from which we obtain:

$$\xi = -\eta \cdot \operatorname{tg} \alpha - \frac{h}{2 \cdot \cos \alpha} \cdot \varphi. \quad (4)$$

An axial reactive load  $\bar{q}_H$  occurs in linear stiff connection. Projections of this load in the direction of the main inertia axes  $y, z$  are:

$$\bar{q}_y = \bar{q}_H \cdot \cos \alpha \quad (5a)$$

$$\bar{q}_z = \bar{q}_H \cdot \sin \alpha. \quad (5b)$$

The total load per unit length of the beam in the direction of the main inertia axes:

$$q_y = -q_v \cdot \sin \alpha + \bar{q}_H \cdot \cos \alpha \quad (6a)$$

$$q_z = q_v \cdot \cos \alpha + \bar{q}_H \cdot \sin \alpha. \quad (6b)$$

The reactive torsional moment is:

$$\bar{m} = -C_D \cdot \varphi + \frac{h}{2} \cdot \bar{q}_H. \quad (7)$$

In this case, the differential equations of equilibrium for the beam assume the following form:

$$E \cdot I_y \cdot \eta^{IV} - q_v \cdot \cos \alpha = \bar{q}_H \cdot \sin \alpha \quad (8)$$

$$E \cdot I_z \cdot \xi^{IV} + q_v \cdot \sin \alpha = \bar{q}_H \cdot \cos \alpha \quad (9)$$

$$E \cdot I_\omega \cdot \varphi^{IV} - G \cdot I_t \cdot \varphi'' + C_D \cdot \varphi - \frac{h}{2} \cdot \bar{q}_H = 0. \quad (10)$$

By applying expressions (4) and (9), Eq. (8) and Eq. (10) can be presented in the following form:

$$\eta^{IV} + \frac{I_z}{I_y + I_z \cdot \operatorname{tg}^2 \alpha} \cdot \frac{h \cdot \sin \alpha}{2 \cdot \cos^2 \alpha} \cdot \varphi^{IV} - \frac{q_v}{E \cdot (I_y + I_z \cdot \operatorname{tg}^2 \alpha) \cdot \cos \alpha} = 0 \quad (11)$$

$$\begin{aligned} & E \cdot \left( I_\omega + I_z \cdot \frac{h^2}{4 \cdot \cos^2 \alpha} - \frac{I_z^2}{I_y + I_z \cdot \operatorname{tg}^2 \alpha} \cdot \frac{h^2 \cdot \sin^2 \alpha}{4 \cdot \cos^4 \alpha} \right) \cdot \varphi^{IV} - G \cdot I_t \cdot \varphi'' + C_D \cdot \varphi = \\ & = q_v \cdot \frac{h}{2} \cdot \operatorname{tg} \alpha \cdot \left[ 1 - \frac{I_z}{(I_y + I_z \cdot \operatorname{tg}^2 \alpha) \cdot \cos^2 \alpha} \right] \end{aligned} \quad (12)$$

After solving Eq. (12) referring to the torsion problem and determining the function  $\varphi(x)$ , Eq. (11) can be solved, which describes the in-plane bending x-z and thus the function  $\eta(x)$  shall be determined. When the functions  $\varphi(x)$  and  $\eta(x)$  are defined, the function  $\xi(x)$  that refers to the main in-plane bending x-y can be determined from the expression (4).

In Eq. (11) and Eq. (12),  $I_y$  and  $I_z$  are the main axial moments of inertia, and  $I_t$  is the torsional moment of inertia (Saint-Venant torsional constant) of the cross section determined by expression:

$$I_t = \frac{1}{3} \int_s t^3 \cdot ds. \quad (13)$$

$I_\omega$  is the main sectorial moment of inertia of the cross section and is defined as [5, 16, 18]:

$$I_\omega = \int_A \omega^2 \cdot dA \quad (14)$$

where  $\omega$  represents the main sectorial coordinate (warping function).

The total moment of torsion  $M_t$  in the cross-section of a beam is equal to the sum of moments of pure torsion (the Saint Venant torsion moment)  $M_{ts}$  and the warping torsion moment  $M_\omega$  of warping torsion [20]:

$$M_t = M_{ts} + M_\omega. \quad (15)$$

The Saint Venant torsion moment is defined by expression [22]:

$$M_{ts} = G \cdot I_t \cdot \varphi' . \quad (16)$$

Saint Venant torsion shear stresses  $\tau_s$  are distributed along the beam wall thickness according to the linear principle and are defined by expression [20, 22, 23]:

$$\tau_s = 2 \cdot \frac{M_{ts}}{I_t} \cdot n \quad (17)$$

where  $n$  is the distance of the observed cross-sectional point from the central plane in the direction of the normal  $\vec{n}$ . The warping torsion moment [20, 22, 23]:

$$M_\omega = -E \cdot I_\omega \cdot \varphi''' . \quad (18)$$

At warping torsion, shear stresses due to warping  $\tau_\omega$  are uniformly distributed along the beam wall thickness and are defined by expression [20, 22, 23]:

$$\tau_\omega = -\frac{M_\omega \cdot \bar{S}_\omega}{I_\omega \cdot t} . \quad (19)$$

$\bar{S}_\omega$  is the sectorial static moment of the cut-off part of cross-section defined by the expression [18, 20, 21]:

$$\bar{S}_\omega = \int_A \omega \cdot dA . \quad (20)$$

Bimoment is defined by the expression [23]:

$$B_\omega = -E \cdot I_\omega \cdot \varphi'' . \quad (21)$$

At warping torsion, direct stresses due to warping are defined by expression:

$$\sigma_\omega = \frac{B_\omega}{I_\omega} \cdot \omega \quad (22)$$

and according to the supposition they are uniformly distributed along the beam wall thickness. The total normal bending stress in the main planes x-y and x-z and the warping torsion are obtained by superposition:

$$\sigma_x = \sigma = \frac{M_y}{I_y} \cdot z - \frac{M_z}{I_z} \cdot y + \frac{B_\omega}{I_\omega} \cdot \omega . \quad (23)$$

The components of shear stress  $\tau_0$  from the transverse force and warping torsion are uniformly distributed along the beam wall thickness and are defined by superposition:

$$\tau_0(x, s) = -\frac{T_z \cdot \bar{S}_y}{I_y \cdot t} + \frac{T_y \cdot \bar{S}_z}{I_z \cdot t} - \frac{M_\omega \cdot \bar{S}_\omega}{I_\omega \cdot t} \quad (24)$$

where  $\bar{S}_y$  and  $\bar{S}_z$  are static moments of the cut-off part of the cross section with respect to the main central axes of inertia y, z.

For the thin-walled beam Z 200/60/15/2, Figure 2, follows:  $\alpha=14.75^0$ ;  $I_y=446.36 \text{ cm}^4$ ;  $I_z=22.98 \text{ cm}^4$ ;  $I_\omega=3629.57 \text{ cm}^6$ ;  $I_t=9.33 \cdot 10^{-2} \text{ cm}^4$ ;  $E=2.33 \cdot 10^5 \text{ MPa}$ ;  $\nu=0.31$ . For the thin-walled beam subjected to the gravity load, rotational stiffness of rotational spring  $C_D$  is

obtained according to Eurocode 3, EN 1993-1-3:2006, section 10.1.5.1. [16]. Models were made and used to determine the rotational stiffness  $C_{D,A}$  provided by trapezoidal sheet T53/162, 5/1 which was connected with wider flange over dents with the thin-walled Z-section 200/60/15/2 beam, Figure 4.

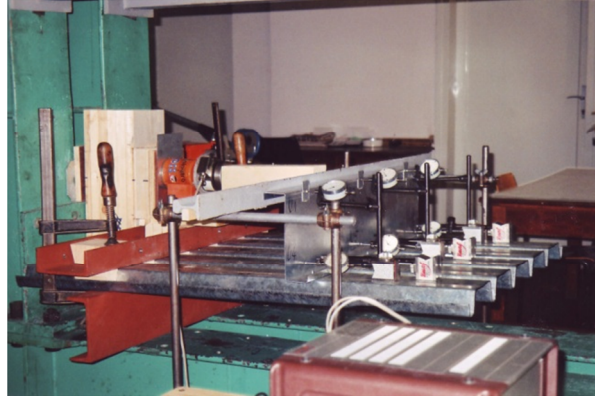


Fig. 4 Experimental determination of rotational stiffness  $C_{D,A}$

Corresponding rotational stiffness of steel sheeting and beam connection for gravity load is  $C_{D,A}=2.64$  kN/m. Rotational stiffness  $C_{D,C}$ , which corresponds to bending stiffness of steel sheeting (flexural stiffness) for sheet over one field with a span (distance between thin-walled beams)  $s=2$  m, is  $C_{D,C}=122.71$  kN/m. Total rotational stiffness of rotational spring obtained in the experiment is  $C_D=2.58$  kN/m, according to Eurocode 3.

In structural analysis, it is often necessary to determine the geometrical properties of thin-walled beam with open cross-section [24, 25]. For the Z-section 200/60/15/2, the diagram of the main sectorial coordinate  $\omega$  is shown in Figure 5(a). The diagram of sectorial static moment of the cut-off part of section  $\bar{S}_\omega$  is shown in Figure 5(b).

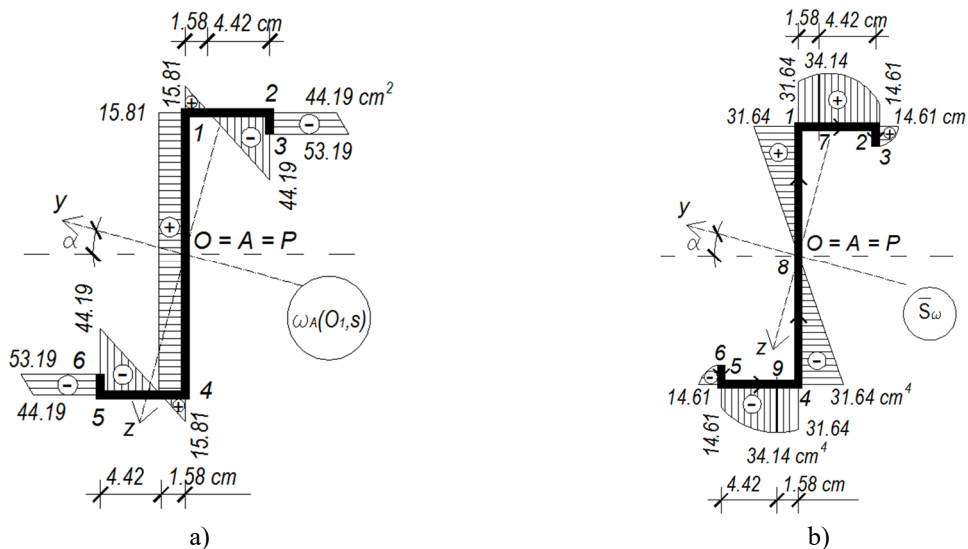


Fig. 5 Diagram of geometrical characteristics of Z-profile: a) diagram of the main sectorial coordinate, b) diagram of the sectorial static moment of the cut-off part of section

For a given value, the differential equation of torsion (12) is reduced to the form:

$$\varphi^{IV} - 0.05859 \cdot \varphi'' + 1.82178 \cdot \varphi = 1.75708 \cdot 10^{-5} \cdot q_v \tag{25}$$

The ends of the beam are freely supported and the rotation around the longitudinal axis is not possible. The boundary conditions are as follows:

when  $x = 0$ :  $\varphi(0) = 0$  ;  $\varphi''(0) = 0$  , when  $x = l$ :  $\varphi(l) = 0$  ;  $\varphi''(l) = 0$ . (26)

For the given boundary conditions (26), the general solution of Eq. (25) is:

$$\varphi(x) = (0.20937 \cdot \sin px \cdot sh kx - 1.98452 \cdot \sin px \cdot ch kx + 10.74921 \cdot \cos px \cdot sh kx - 9.64485 \cdot \cos px \cdot ch kx + 9.64485) \cdot 10^{-6} \cdot q_v \tag{27}$$

where

$$k = 0.83037 \left[ \frac{1}{m} \right] ; p = 0.81254 \left[ \frac{1}{m} \right]. \tag{28}$$

The ends of the beam are freely supported. The boundary conditions for the function  $\eta(x)$  in Eq. (11) are:

when  $x = 0$ :  $\eta(0) = 0$  ;  $\eta''(0) = 0$  , when  $x = l$ :  $\eta(l) = 0$  ;  $\eta''(l) = 0$ . (29)

For the given boundary conditions (26) and (29), the general solution of Eq. (11) is:

$$E \cdot (I_y + I_z \cdot tg^2 \alpha) \cdot \eta = -E \cdot I_z \cdot \frac{h \cdot \sin \alpha}{2 \cdot \cos^2 \alpha} \cdot \varphi + \frac{q_v}{\cos \alpha} \cdot \frac{x^4}{24} - \frac{q_v}{\cos \alpha} \cdot \frac{l}{12} \cdot x^3 + \frac{q_v}{\cos \alpha} \cdot \frac{l^3}{24} \cdot x \tag{30}$$

Function  $\xi(x)$  is determined by the expression (4) and the Eq. (27) and Eq. (30). Total deflection in the middle of the girder span (total shear centre displacement, apropos centre of gravity of cross- section displacement) for load  $q_v=2.5$  kN/m:

$$f_u \left( \frac{l}{2} \right) = \sqrt{\eta^2 \left( \frac{l}{2} \right) + \xi^2 \left( \frac{l}{2} \right)} = 3.84 \text{ mm}. \tag{31}$$

For load  $q_v=2.5$  kN/m, the diagram of total normal cross-section stresses in the centre span of the beam ( $x=l/2$ ) is shown in Figure 6(a), and the diagram of the full shear stress in the cross section next to the beam support ( $x=0$ ) is shown in Figure 6(b).

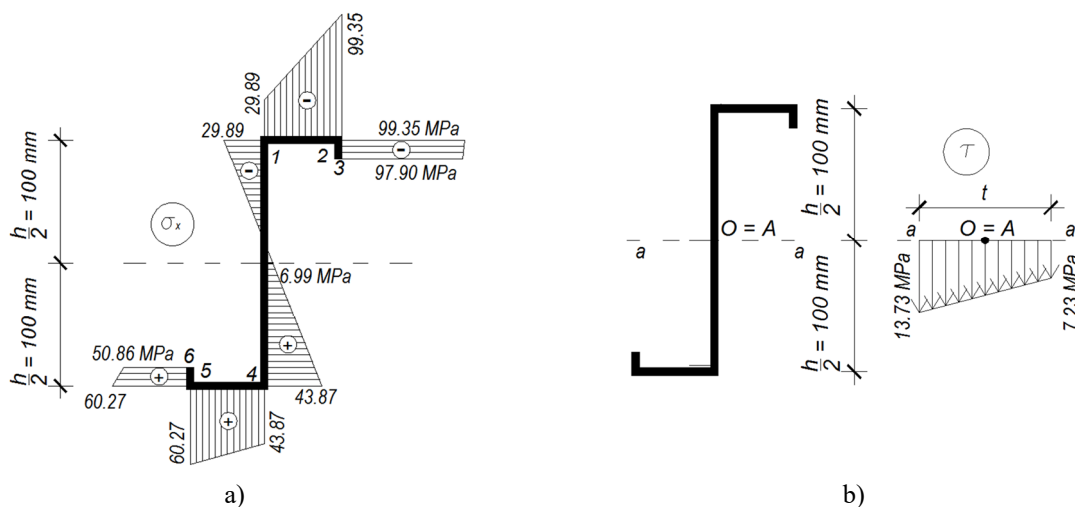


**Fig. 6** Diagrams of stresses: a) normal cross-section stresses in the centre span of the beam ( $x=l/2$ ), b) full shear stress in the cross-section next to the beam support ( $x=0$ )

**3. Thin-walled Z-section beam laterally restrained by linear stiff connection (Model “B”)**

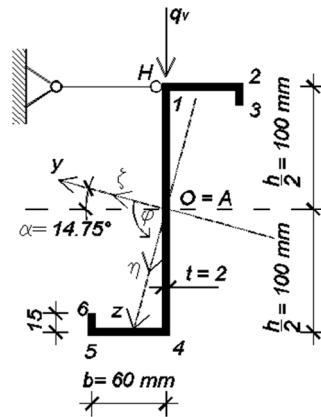


**Fig. 7** Thin-walled Z-section beam laterally restrained by linear stiff connection (Model “B”)

Beam is restrained with linear stiff connection in the point H, Fig. 7. Displacement of the point H in the direction of linear stiff connection is shown by expression (3), and component of the shear centre displacement  $\xi$  is given by the expression (4). Displacement of the point H in the direction perpendicular to the linear stiff connection is determined as follows:

$$\delta_v = -\xi \cdot \sin \alpha + \eta \cdot \cos \alpha . \tag{32}$$

An axial reactive load  $\bar{q}_H$  occurs in linear stiff connection. The load’s projections in the direction of the main inertia axes y and z are:

$$q_y = \bar{q}_H \cdot \cos \alpha \tag{33a}$$

$$q_z = \bar{q}_H \cdot \sin \alpha . \tag{33b}$$

The total load per length unit of the beam in the direction of the main inertia axes is shown with Eq. (6a) and Eq. (6b). The reactive torsional moment is:

$$\bar{m} = \frac{h}{2} \cdot \bar{q}_H . \tag{34}$$

The differential equations of equilibrium for the beam assume the following form:

$$E \cdot I_y \cdot \eta^{IV} - q_v \cdot \cos \alpha = \bar{q}_H \cdot \sin \alpha \tag{35}$$

$$E \cdot I_z \cdot \xi^{IV} + q_v \cdot \sin \alpha = \bar{q}_H \cdot \cos \alpha \tag{36}$$

$$E \cdot I_\omega \cdot \varphi^{IV} - G \cdot I_t \cdot \varphi'' - \frac{h}{2} \cdot \bar{q}_H = 0 . \tag{37}$$

Once we put the expression (4) in Eq. (36) we get:

$$-E \cdot I_z \cdot \text{tg} \eta^{IV} - E \cdot I_z \cdot \frac{h}{2 \cdot \cos \alpha} \cdot \varphi^{IV} + q_v \cdot \sin \alpha = \bar{q}_H \cdot \cos \alpha \tag{38}$$

From the Eq. (38) follows:

$$\bar{q}_H = -E \cdot I_z \cdot \frac{\sin \alpha}{\cos^2 \alpha} \cdot \eta^{IV} - E \cdot I_z \cdot \frac{h}{2 \cdot \cos^2 \alpha} \cdot \varphi^{IV} + q_v \cdot \operatorname{tg} \alpha \quad (39)$$

When we put Eq. (39) into Eq. (35) and Eq. (37) we get:

$$E \cdot (I_y + I_z \cdot \operatorname{tg}^2 \alpha) \cdot \eta^{IV} + E \cdot I_z \cdot \frac{h \cdot \sin \alpha}{2 \cdot \cos^2 \alpha} \cdot \varphi^{IV} - \frac{q_v}{\cos \alpha} = 0 \quad (40)$$

$$E \cdot \left( I_\omega + I_z \cdot \frac{h^2}{4 \cdot \cos^2 \alpha} \right) \cdot \varphi^{IV} - G \cdot I_t \cdot \varphi'' + E \cdot I_z \cdot \frac{h \cdot \sin \alpha}{2 \cdot \cos^2 \alpha} \cdot \eta^{IV} = q_v \cdot \frac{h}{2} \cdot \operatorname{tg} \alpha \quad (41)$$

Eq. (40) can be written as follows:

$$\eta^{IV} + \frac{I_z}{I_y + I_z \cdot \operatorname{tg}^2 \alpha} \cdot \frac{h \cdot \sin \alpha}{2 \cdot \cos^2 \alpha} \cdot \varphi^{IV} - \frac{q_v}{E \cdot (I_y + I_z \cdot \operatorname{tg}^2 \alpha) \cdot \cos \alpha} = 0 \quad (42)$$

If we put the expression for  $\eta^{IV}$  given from the Eq. (42) into Eq. (41), we get:

$$\begin{aligned} E \cdot \left( I_\omega + I_z \cdot \frac{h^2}{4 \cdot \cos^2 \alpha} - \frac{I_z^2}{I_y + I_z \cdot \operatorname{tg}^2 \alpha} \cdot \frac{h^2 \cdot \sin^2 \alpha}{4 \cdot \cos^4 \alpha} \right) \cdot \varphi^{IV} - G \cdot I_t \cdot \varphi'' = \\ = q_v \cdot \frac{h}{2} \cdot \operatorname{tg} \alpha \cdot \left[ 1 - \frac{I_z}{(I_y + I_z \cdot \operatorname{tg}^2 \alpha) \cdot \cos^2 \alpha} \right] \end{aligned} \quad (43)$$

After solving Eq. (43) referring to the torsion problem and determining the function  $\varphi(x)$ , Eq. (40) and Eq. (42) can be solved. For certain functions  $\varphi(x)$  and  $\eta(x)$ , the reactive load  $\bar{q}_H$  in the linear connection can be determined by the Eq. (39), and the component of the shear centre displacement  $\xi$ , that refers to the main in-plane bending x-y can be determined by the expression (36). Thereby the expression (4) is used to verify correctness of the obtained results of functions  $\varphi(x)$ ,  $\eta(x)$  and  $\xi(x)$ .

For the given values, differential torsion Eq. (43) is reduced to the following form:

$$\varphi^{IV} - 0.05859 \cdot \varphi'' = 1.75708 \cdot 10^{-5} \cdot q_v \quad (44)$$

The ends of the beam are freely supported and the rotation around the longitudinal axis is not possible. Boundary conditions are given by Eq. (26). For the given boundary conditions (26), a general solution of the Eq. (44) is:

$$\varphi(x) = 10^{-2} \cdot q_v \cdot \left( -0.50648 + 0.04102 \cdot x + 0.17174 \cdot e^{0.24269 \cdot x} + 0.33474 \cdot e^{-0.24269 \cdot x} - 0.01492 \cdot x^2 \right) \quad (45)$$

The ends of the beam are freely supported. Boundary conditions for the function  $\eta(x)$  in the Eq. (42) are determined by the Eq. (29). For the given boundary conditions (26) and (29), a general solution of the Eq. (42) is:

$$\begin{aligned} \eta(x) = \left( -0.02398 \cdot 10^{-4} \cdot e^{0.24269 \cdot x} - 0.04675 \cdot 10^{-4} \cdot e^{-0.24269 \cdot x} + 4.1281 \cdot 10^{-8} \cdot x^4 - \right. \\ \left. - 0.02270 \cdot 10^{-5} \cdot x^3 + 0.02083 \cdot 10^{-5} \cdot x^2 + 0.02855 \cdot 10^{-5} \cdot x + 0.70740 \cdot 10^{-5} \right) \cdot q_v \end{aligned} \quad (46)$$

Function  $\xi(x)$  is determined by the expression (4), Eq. (45) and Eq. (46). Total deflection in the middle of the girder span (total shear centre displacement, apropos centre of gravity of cross-section displacement) for load  $q_v=2.5$  kN/m:

$$f_u\left(\frac{l}{2}\right) = \sqrt{\eta^2\left(\frac{l}{2}\right) + \xi^2\left(\frac{l}{2}\right)} = 3.84 \text{ mm}.$$

For load  $q_v=2.5$  kN/m, the diagram of total normal cross-section stresses in the centre span of the beam ( $x=l/2$ ) is shown in Figure 8(a), and the diagram of the full shear stress in the cross section next to the beam support ( $x=0$ ) is shown in Figure 8(b).

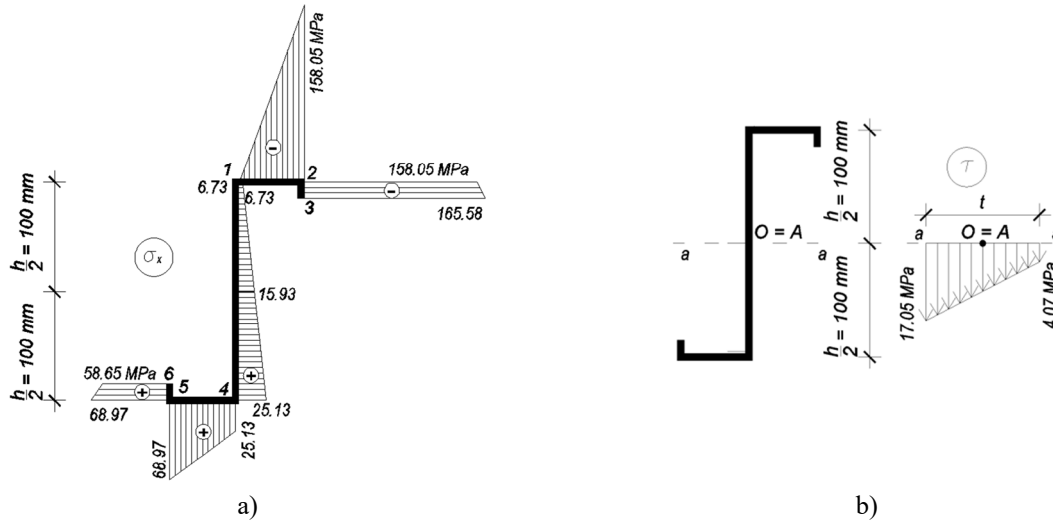


Fig. 8 Diagrams of stresses: a) normal cross-section stresses in the centre span of the beam ( $x=l/2$ ), b) full shear stress in the cross-section next to the beam support ( $x=0$ )

#### 4. Thin-walled Z-section beam laterally restrained by rotary elastic connection (Model “C”)

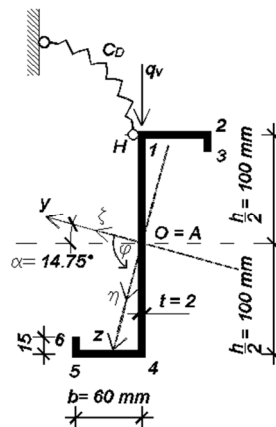


Fig. 9 Thin-walled Z-section beam laterally restrained by rotary elastic connection (Model “C”)

The beam is restrained by rotary elastic connection in the point H, Figure 9. The differential equations of equilibrium for the beam assume the following form:

$$E \cdot I_y \cdot \eta^{IV} - q_v \cdot \cos \alpha = 0 \tag{47}$$

$$E \cdot I_z \cdot \xi^{IV} + q_v \cdot \sin \alpha = 0 \tag{48}$$

$$E \cdot I_\omega \cdot \varphi^{IV} - G \cdot I_t \cdot \varphi'' + C_D \cdot \varphi = 0. \tag{49}$$

Boundary conditions for the function  $\eta(x)$  are given by the Eq. (29). For the given boundary conditions (29), a general solution of the Eq. (47) is:

$$\eta(x) = \frac{q_v \cdot \cos \alpha}{E \cdot I_y} \left( \frac{x^4}{24} - \frac{l \cdot x^3}{12} - \frac{l^3 \cdot x}{12} \right). \quad (50)$$

The bending moment around the y axis:

$$M_y = -E \cdot I_y \cdot \frac{d^2 \eta}{dx^2}. \quad (51)$$

Boundary conditions for the function  $\xi(x)$  are:

$$\text{when } x = 0: \xi(0) = 0; \xi''(0) = 0, \text{ when } x = l: \xi(l) = 0; \xi''(l) = 0. \quad (52)$$

For the given boundary conditions, a general solution of the Eq. (48) is:

$$\xi(x) = -\frac{q_v \cdot \sin \alpha}{E \cdot I_z} \left( \frac{x^4}{24} - \frac{l \cdot x^3}{12} - \frac{l^3 \cdot x}{12} \right) \quad (53)$$

The bending moment around the z axis:

$$M_z = -E \cdot I_z \cdot \frac{d^2 \xi}{dx^2} \quad (54)$$

The ends of the beam are leaning freely, and the rotation around the longitudinal axis is not possible. Boundary conditions for the function  $\varphi(x)$  are given by the Eq. (26). For the given boundary conditions (26), a general solution of the Eq. (49) is:

$$\varphi(0) = 0. \quad (55)$$

As follows, there is no rotation of the cross section around the x axis, because the total external load goes through the shear centre of the beams cross section. Rotary elastic connection isn't activated, and the beam acts as a beam without lateral restraints. The state of stress and strain fully corresponds to the state of stress and strain of beams without lateral restraints as model "D".

## 5. Thin-walled Z-section beam without lateral restraints (Model "D")

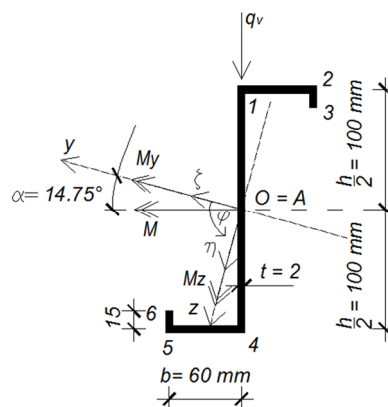


Fig. 10 Thin-walled Z-section beam without lateral restraints (Model "D")

Since the load acts in the shear centre "A", the beam is exposed only to oblique bending, without torsion, Figure 10, [26, 27]. The differential equations of equilibrium for the beam assume the following form:

$$E \cdot I_y \cdot \eta^{IV} - q_v \cdot \cos \alpha = 0 \tag{56}$$

$$E \cdot I_z \cdot \xi^{IV} + q_v \cdot \sin \alpha = 0 \tag{57}$$

Normal stresses in cross section:

$$\sigma_x = \frac{M_y}{I_y} \cdot z - \frac{M_z}{I_z} \cdot y = \frac{q_v \cdot l^2 \cdot \cos \alpha}{8} \cdot \frac{z}{I_y} - \frac{q_v \cdot l^2 \cdot \sin \alpha}{8} \cdot \frac{y}{I_z} \tag{58}$$

The diagram of total normal cross-section stresses  $\sigma_x$  in the centre span of the beam ( $x=l/2$ ) is shown in Figure 11(a).

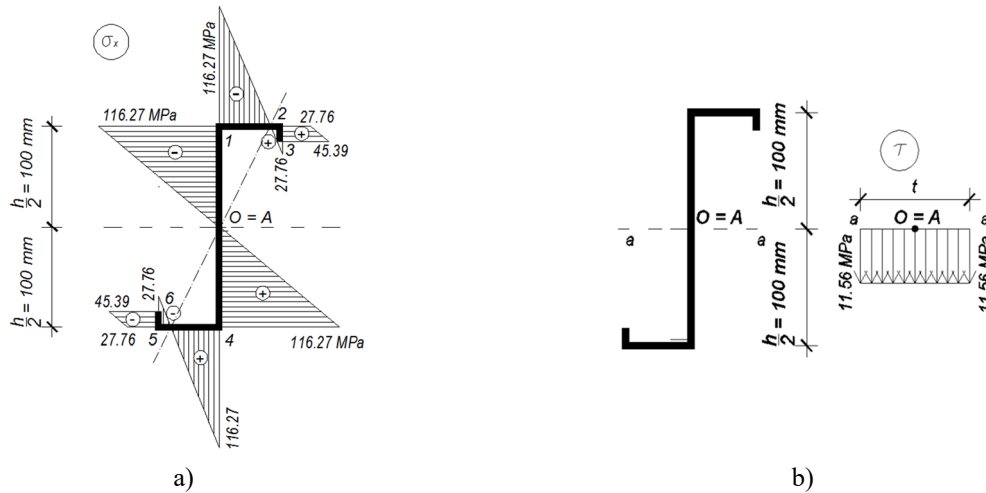


**Fig. 11** Diagrams of stresses: a) normal cross-section stresses in the centre span of the beam ( $x=l/2$ ), b) full shear stress in the cross-section next to the beam support ( $x=0$ )

Shear stresses  $\tau_0$  from the transverse force are uniformly distributed along the beam wall thickness and are defined by expression:

$$\tau_0(x, s) = -\frac{T_z \cdot \bar{S}_y}{I_y \cdot t} + \frac{T_y \cdot \bar{S}_z}{I_z \cdot t} \tag{59}$$

The diagram of the full shear stress in the cross section next to the beam support ( $x=0$ ) is shown in Fig. 11(b).

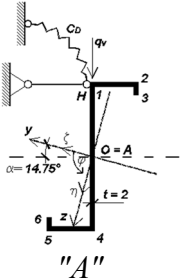
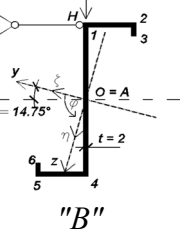
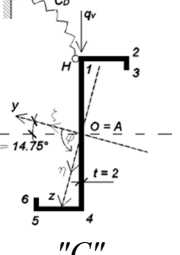
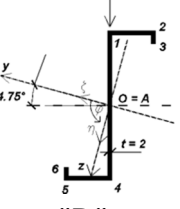
Total deflection in the middle of span ( $x=l/2$ ) is:

$$f_u\left(\frac{l}{2}\right) = \sqrt{\eta^2\left(\frac{l}{2}\right) + \xi^2\left(\frac{l}{2}\right)} = \sqrt{\left(\frac{5 \cdot q_v \cdot \sin \alpha \cdot l^4}{384 \cdot E \cdot I_z}\right)^2 + \left(\frac{5 \cdot q_v \cdot \cos \alpha \cdot l^4}{384 \cdot E \cdot I_y}\right)^2} = 9.02 \text{ mm} \tag{60}$$

## 6. Conclusion

A review of the extreme values of total normal cross-section stresses in the centre span of the beam ( $x=l/2$ ), full shear stresses in the cross section next to the beam support ( $x=0$ ), and deflections in the centre span of the beam are shown in Table 1.

**Table 1** Comparison of the research results

MODEL	$f(l/2)$	$ \sigma_x _{\max}$	$ \tau_x _{\max}$
	mm	MPa	MPa
 <p>"A"</p>	3.84	99.35	13.73
 <p>"B"</p>	4.11	165.58	17.05
 <p>"C"</p>	9.02	116.27	11.56
 <p>"D"</p>	9.02	116.27	11.56

From the comparison of the results of the research, it can be concluded that deflections and normal stresses are the lowest in the model "A". Shear stresses are the lowest in the models "C" and "D", because there isn't any impact of the warping torsion. Normal stresses and shear stresses are the highest in the model "B" due to the high impact of the warping torsion, which is considerably higher than in the model "A". In the model "B" normal stresses from warping torsion in the most stressed point 3 of the cross-section in the centre span of the beam are  $\sigma_{\omega} = -53.61$  MPa and are about one-third of total maximum stress  $\sigma_x = -165.58$  MPa in the point 3 of the cross section. From the analysis of the research follows that, depending on the variant of the lateral restraints of thin-walled beams, lateral restraint may reduce stress and strain, but it may also increase stress in thin-walled beam.

**REFERENCES**

[1] Z.M. Ye, R. Kettle and L.Y. Li: Analysis of cold-formed zed-purlins partially restrained by steel sheeting, *Comput Struct*, 82, 9-10, 2004, 731-739  
 [2] Z.M. Ye, R. Kettle and L.Y. Li and B. W. Schafer: Buckling behavior of cold-formed zed-purlins partially restrained by steel sheeting, *Thin Wall Struct*, 40, 10, 2002, 853-864

- [3] C. Ren, L.Y. Li and J. Yang: Bending analysis of partially restrained channel-section purlins subjected to up-lift loadings, *J Constr Steel Res*, 72, 5, 2012, 254-260
- [4] F. McCann, L. Gardner and M.A. Wade: Design of steel beams with discrete lateral restraints, *J Constr Steel Res*, 80, 1, 2013, 82-90
- [5] V.Z. Vlasov: Thin-Walled Elastic Beams, 2nd edition, Jerusalem, Israel; Program for Translations; 1961.
- [6] Y.L. Pi, B.M. Put and N.S. Trahair: Lateral buckling strengths of cold-formed Z-section beams, *Thin Wall Struct*, 34, 1, 1999, 65-93
- [7] K. Magnucki, W. Szyc and P. Stasiewicz: Stress state and elastic buckling of a thin walled beam with monosymmetrical open cross-section, *Thin Wall Struct*, 42, 1, 2004, 25-38
- [8] R. Pavazza, A. Matoković and B. Plazibat: Torsion of thin-walled beams of symmetrical open cross-sections with influence of shear, *Transactions of Famena*, 37, 2, 2013, 1-14.
- [9] R. Pavazza, A. Matoković and B. Plazibat: Bending of thin-walled beams of symmetrical open cross-sections with influence of shear, *Transactions of Famena*, 37, 3, 2013, 17-30.
- [10] D. Šimić: Modelling of load transfer to laterally restrained thin-walled beams with open cross-section, *Transactions of Famena*, 34, 3, 2010, 47-56.
- [11] X.T. Chu, J. Rickard, and L.Y. Li: Influence of lateral restraint on lateral-torsional buckling of cold-formed steel purlins, *Thin Wall Struct*, 43, 5, 2005, 800-810
- [12] T. Gao and C.D. Moen: Predicting rotational restraint provided to wall girts and roof purlins by through-fastened metal panels, *Thin Wall Struct*, 61, 12, 2012, 145-153
- [13] A.S.J. Foster and L. Gardner: Ultimate behaviour of steel beams with discrete lateral restraints, *Thin Wall Struct*, 72, 11, 2013, 88-101
- [14] R. Pavazza, S. Jović: A comparison of approximate analytical methods and the finite element method in the analysis of short clamped thin-walled beams subjected to bending by uniform loads, *Transactions of Famena*, 31, 1, 2007, 37-54.
- [15] R. Pavazza, S. Jović: A Comparison of the Analytical Methods and the Finite Method in the Analysis of Short Thin-walled Beams Subjected to Bending by Couples, *Transactions of Famena*, 30, 2, 2006, 21-30.
- [16] Eurocode 3, *Design of Steel Structures-Part 1-3: General Rules-Supplementary Rules for Cold Formed Thin Gauge Members and Sheeting*, European Committee for Standardization, 2006.
- [17] B.W. Schafer, R.H. Sangree and Y. Guan: Experiments on rotational restraint of sheathing, Report for American Iron and Steel Institute-Committee on Framing Standards. Baltimore, Maryland, USA, 2007.
- [18] A. Gjelsvik: The theory of thin walled bars, New York, John Wiley&Sons, 1981.
- [19] J.F. Doyle: Nonlinear Analysis of Thin-Walled Structures, Statics, Dynamics and Stability, Springer-Verlag, New York, NY, USA, Inc. 2001.
- [20] D. Šimić: The Theory of Thin-Walled Beams with Open Cross Section, Faculty of civil engineering, University of Zagreb, Manualia Universitatis studiorum Zagrabiensis, Zagreb, Croatia, 2008.
- [21] D. Šimić: Analysis of Laterally Restrained Thin-Walled Open Section Beams, *Građevinar* 56, 5, 2004, 277- 287.
- [22] M. Ojalvo: Thin-walled bars with open profiles, The Olive Press, Estes Park, Colorado, 1991.
- [23] N.W. Murray: Introduction to the Theory of Thin-Walled Structures, Oxford University Press, New York, 1986.
- [24] R. Pavazza: Introduction to analysis of thin-walled beams, Kingen, Zagreb, 2007.
- [25] B. Plazibat, A. Matoković: A Computer Program for Calculating Geometrical Properties of Symmetrical Thin-Walled Cross-Section, *Transactions of Famena*, 35, 4, 2011, 65-84.
- [26] D. Šimić Penava, A. Radić and T. Ilijaš: Elastic stability analysis of the thin-walled C- and Z-section beams without lateral restraints, *Transactions of Famena*, 38, 2, 2014, 41-52.
- [27] M. Math: Finite element study and simulation of plate bending process, *Journal of Simulation Modelling*, 1, 1, 2002, 31-40.

Submitted: 22.12.2014

Accepted: 14.10.2015

Diana Šimić Penava\*  
 Domagoj Damjanović  
 Tanja Ilijaš  
 University of Zagreb, Faculty of Civil  
 Engineering  
 Kačićeva 26, Zagreb, Croatia  
 \*corresponding author, e-mail:  
 dianas@grad.hr